Progress In Electromagnetics Research C, Vol. 34, 253–263, 2013

A COMPOSITE DIPOLE ANTENNA ARRAY WITH DIRECT FEED

S. Lin*, Y.-C. Lin, X. Liu, M.-Q. Liu, X.-R. Ma, and L.-W. Jing

School of Electronics and Information Engineering, Harbin Institute of Technology, Harbin 150080, China

Abstract—Design of a composite dipole antenna array with direct feed is presented. In the form of printed-circuit antennas, the structure of the design consists of a doublet antenna and an elliptic loaded monopole antenna with a skirted dipole. As the load of the antenna array, this elliptic monopole provides wider bandwidth. Therefore, with the load possessing a radiation characteristic, it contributes to enhancing efficiency of the antenna array and hence the omni-directional radiation gain. A good agreement between simulated results by CST Microwave Studio® and tested results suggests that the reflection coefficient for the frequency range between 4.35 GHz to 5.0 GHz is lower than −10 dB. The out-of-roundness on H-plane is lower than 2 dB and the maximum gain is higher than 6 dB for the frequency range from 4.6 to 5.0 GHz. What is more, the gain per wavelength is about 4 dB, showing the antenna's excellence in miniaturization.

1. INTRODUCTION

For point-to-multipoint communication systems, there are common requirements for base station antennas to possess the characteristics of high-gain, wide-band and omni-directional, so terminal antennas are required to be capable of both miniature and omni-directional, such as the mobile communication of base stations with terminal users. Generally, an omni-directional antenna is designed to be higher than 4 dBi in gain, which accordingly guarantees link gain and beam coverage. Additionally, an antenna is expected to meet the needs of both miniaturization and wider bandwidth. The former

Received 12 October 2012, Accepted 23 November 2012, Scheduled 25 November 2012

* Corresponding author: Shu Lin (linshu@hit.edu.cn).

aims to miniaturize communication systems and the latter accelerates communication rate, together with securing communal applications of antennas in multi-system as well as serving as an important means of antenna miniaturization.

According to indexes demanded above, researchers proposed a vast deal of plans of antenna designs that can be divided into following two categories: ultra-wideband radiating antenna elements and high-gain omni-directional antennas. Initially, ultra-wideband radiating antenna elements [1–4] offer an excellent characteristic of a fairly wide range of impedance bandwidth, which can generally reach a ratio more than 2 : 1. However, the antenna radiation pattern bandwidth is relatively narrow and the gain is low. Although these can be reconciled with a means of an array [5, 6], it fails to be operated due to its complexity and large size. Additionally, high-gain omni-directional antennas [7–9], which are based on COCO antenna, provide narrow bandwidth, low omin-directional gain and lower electrical length ratio in the polarization direction, resulting in adverse effects on antenna miniaturization.

A composite dipole planar antenna array with direct feed is presented in this paper. That is, the overall antenna is in the form of printed circuits, consisting of a doublet antenna and an elliptic loaded monopole antenna with a skirted dipole. By simulating the models built by CST Microwave Studio®, we finally got an omni-directional high-gain antenna with its overall omni-directional gain better than 4 dBi over a frequency range of 4.18 to 5.03 GHz (the relative bandwidth is 18.5%). The article is divided into the following five parts: (1) introduction; (2) antenna structure; (3) simulation analysis; (4) tested results; (5) conclusion.

2. ANTENNA STRUCTURE

Figure 1 shows the antenna structure. The entire antenna is a two-sided printed circuit board (PCB), printed on a FR-4 epoxy substrate with 1.5 mm thickness, whose dielectric constant ε_r is 4.4. The black areas printed on both sides of the dielectric slab are metals (Figures 1(a), (b), (c)). A CPW-fed structure is applied to the design. Furthermore, the metals on the left and right on the front of the antenna (as shown in Figure 1(a)) are connected together by the metallic jump wires on the back of the slab through the metalized vias. And the elliptical monopole is located in the antenna terminal. Structure parameters of the antenna are as follows. $R_1 = 14.8\,\mathrm{mm}$, $L = 96.1$, $w_1 = 4\,\mathrm{mm}$, $S = 1.9\,\mathrm{mm}$, $g = 3\,\mathrm{mm}$, $g_1 = 4.9\,\mathrm{mm}$, $l_1 = 1.3\,\mathrm{mm}$, $l_2 = 19.3\,\mathrm{mm}$, $l_3 = 4.7\,\mathrm{mm}$, $l_4 = 19.3\,\mathrm{mm}$, $l_5 = 1.5\,\mathrm{mm}$,

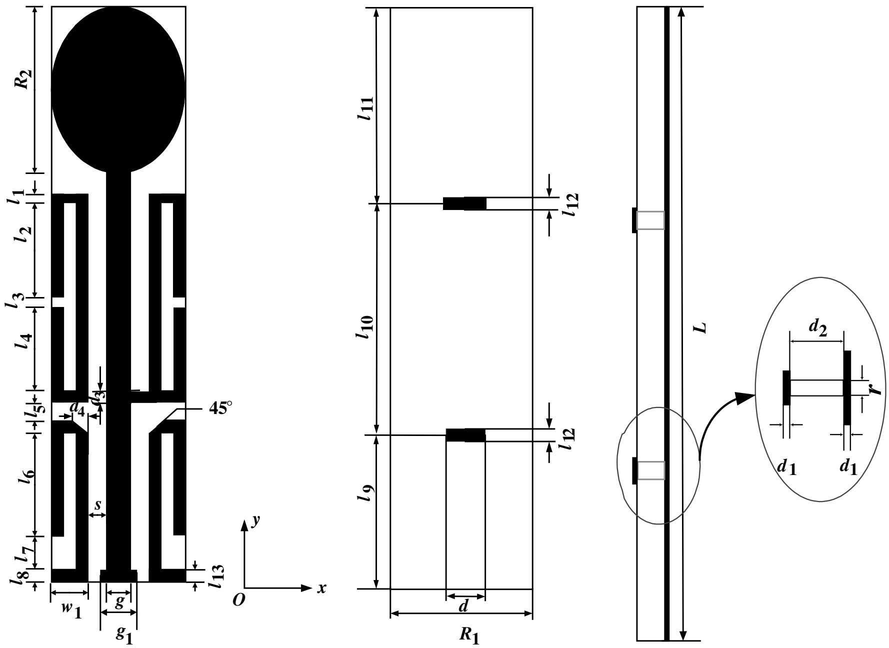

Figure 1. Composite dipole antenna array with direct feed. (a) Front-side, (b) back-side, (c) flank and metalized via.

$l_6 = 19.3\,\text{mm}$, $l_7 = 3\,\text{mm}$, $l_8 = 1.1\,\text{mm}$, $l_9 = 26.85\,\text{mm}$, $l_{10} = 44.6\,\text{mm}$, $l_{11} = 24.65\,\text{mm}$, $l_{12} = 0.4\,\text{mm}$, $R_2 = 22\,\text{mm}$, $d = 8.5\,\text{mm}$, $d_1 = 0.1\,\text{mm}$, $d_2 = 1.5\,\text{mm}$, $d_3 = 1\,\text{mm}$, $d_4 = 1.7\,\text{mm}$, $r = 0.2\,\text{mm}$.

The overall antenna is in the form of PCB, regarded to consist of a doublet antenna (in the lower portion of Figure 1(a)) and an elliptic loaded monopole antenna with a skirted dipole (in the upper half of Figure 1(a)).

3. SIMULATION ANALYSIS

3.1. Impacts of Loaded Sheet Metal Next to the Feeding Port

With the model simulated by CST Microwave Studio® software in Figure 1, results are shown in Figure 2 as well as Figure 3, illuminating reflection coefficient for the frequency range between 4.18 to 5.03 GHz is lower than $-10\,\text{dB}$ and the reflection coefficient here is calculated when port impedance of the design is $85.1\,\Omega$ (Figure 2(a)). It is worth stressing that the loaded sheet metal (Figure 2(b)) next to the feeding

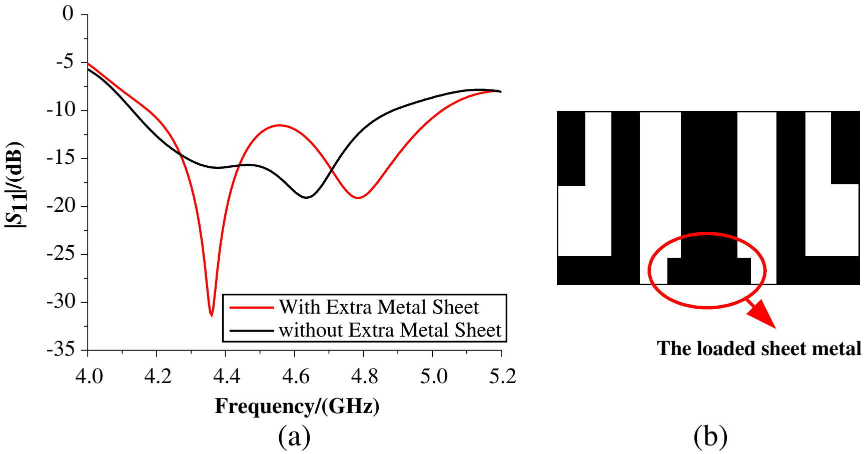

Figure 2. Simulated results of reflection coefficient of the antenna ($|S_{11}|$). (a) Reflection coefficient, (b) schematic diagram of the loaded sheet metal next to the feeding port.

port at the bottom of the antenna plays a crucial role in improving port impedance. Because it is necessary to meet the requirements of omni-directional radiation when designing an antenna in simulation, which leads to fairly fine middle feed, thus port impedance is supposed to be increased. However, as it can be seen from the comparison in Figure 2(a), when sheet metal is added, port impedance decreases from $127.3\,\Omega$ to $85.1\,\Omega$, which ends up with matching SMA connector ($50\,\Omega$) more smoothly. Therefore, the working bandwidth of the antenna increases by 0.1 GHz; that is, a frequency range of 4.18–5.03 GHz substitutes the range of 4.13–4.88 GHz.

3.2. Surface Currents Analysis and Radiation Pattern

Figure 3 shows simulated results of surface current at 4.8 GHz, a typical working frequency point of the antenna. Therefore, we can draw a conclusion that currents capable of radiation are i_1–i_8 in Figure 3, and the rest of currents in transmission lines, with energy limited in CPW, fail to radiate. Figures 4 and 5 present amplitude and phase distributions of currents i_1–i_8 in simulation, respectively.

Figures 4 and 5 show that: (1) in terms of the current amplitudes, each current among i_1–i_8 has both one antinode and two troughs, which is similar to the characteristics of standing waves; (2) the distribution of the phases of i_1–i_8 suggests that each current distributes along y direction (Figure 3). Though in y direction, the overall length L of the design is 96.1 mm, equal to 1.54λ (4.8 GHz), the variation of the

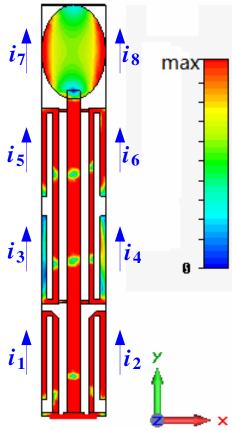

Figure 3. Relative values of surface currents working at a typical frequency point of antenna (4.8 GHz).

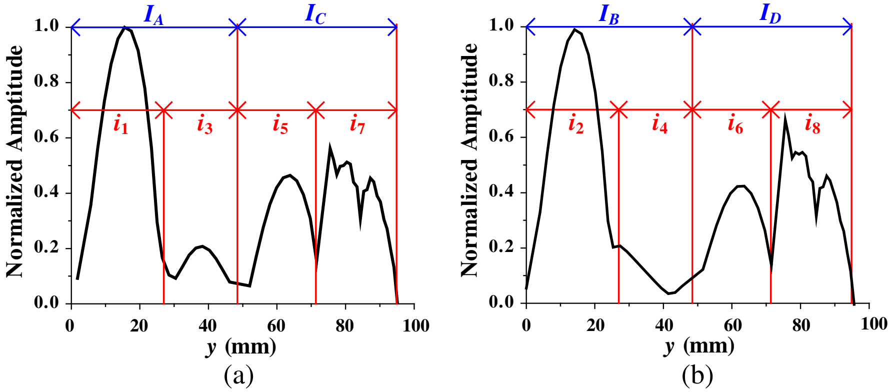

Figure 4. Normalized amplitude distribution of currents i_1–i_8. (a) i_1, i_3, i_5, i_7. (b) i_2, i_4, i_6, i_8.

phases is much less than 360°, which also resembles the features of the standing waves very well. Considering that the dipole antenna is a typical kind of standing wave antenna, we can apply the dipole array model to the interpretation of the radiation characteristics of the antenna.

Currents i_1–i_8 are standing wave currents, which lead to the formation of array (Figure 6), consisting of 4 dipoles (including I_A–I_D shown in Figures 4, 5). Therefore, radiation characteristics of the antenna can be explained by radiation of the array. First, each two standing wave currents are equivalent to a dipole antenna. Among

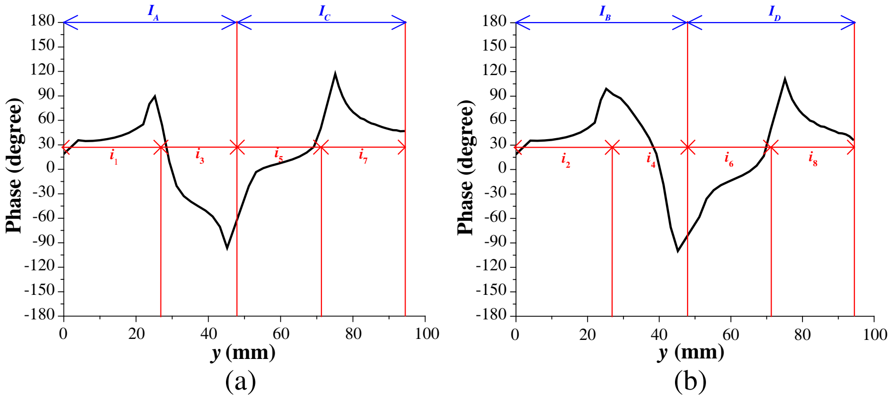

Figure 5. Phase distribution of currents i_1–i_8. (a) i_1, i_3, i_5, i_7. (b) i_2, i_4, i_6, i_8.

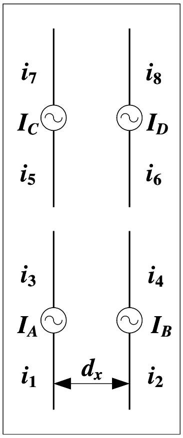

Figure 6. Schematic diagram of equivalent standing wave currents array.

them, I_A and I_B approximately share the same amplitude and phase, which is the same with relationships between I_C and I_D. What is more, the difference of phases between I_A and I_C is little, resulting in the formation of a side-fire array 1. And in the same way, the similarities in both amplitudes and phases of I_B and I_D also lead to the formation of a broadside array 2. These two broadside arrays generate omni-directional radiation on x-z plane and the relatively short distance between them ($d_x = 13.5\,\text{mm} = 0.216\lambda$, $4.8\,\text{GHz}$) contributes to the formation of another omni-directional radiation on x-z plane. On account of broadside arrays action, the overall antenna arrays generate

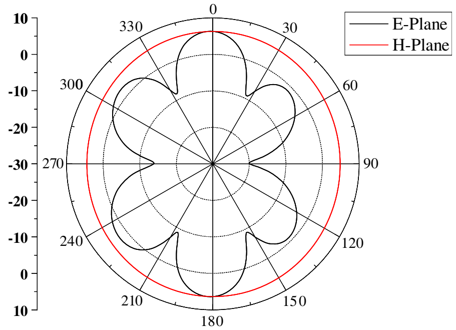

Figure 7. Simulated results of the antenna pattern (4.8 GHz).

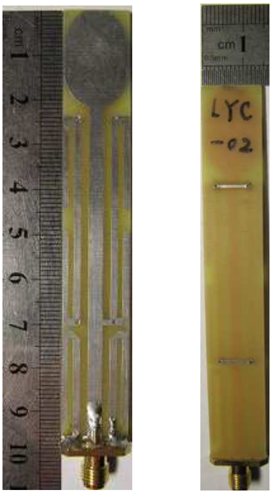

Figure 8. Antenna prototype. (a) Front-side. (b) Back-side.

omni-directional radiation as well as higher gain.

Simulated results of the antenna pattern presented in Figure 7 suggest that omni-directional radiation on x-z plane has been implemented by the design on aspects of out-of-roundness less than 2 dB, and maximum gain being 6.4 dB. So the validity of the analysis in this chapter can be verified by simulated results.

4. TESTED RESULTS

According to sizes of the design, the antenna has been made (Figure 8) and measured by using Agilent E8363B Vector Network Analyzer

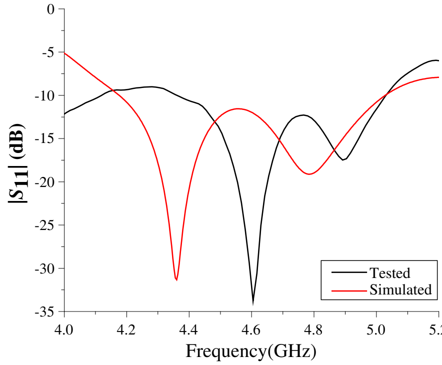

Figure 9. Tested reflection coefficient of antenna.

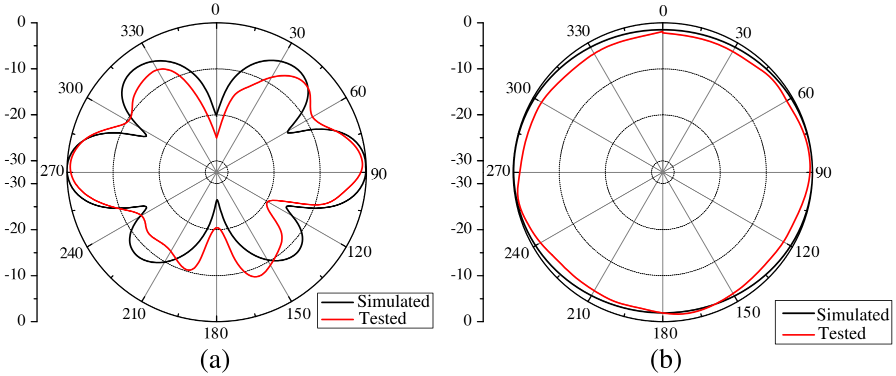

Figure 10. Tested results of antenna pattern (at 4.8 GHz). (a) Tested results of antenna pattern on E-plane (y-z plane), (b) tested results of antenna pattern on H-plane (x-z plane).

in a microwave anechoic chamber. Its tested results are shown in Figures 9 and 10, representing that simulated results are in good agreement with tested results. Therefore, simulated results are verified. Reflection coefficient simulations for the frequency range from 4.2 GHz to 5 GHz (the relative bandwidth is 17.4%) are lower than -10 dB, and the tested results are between 4.35 to 5.0 GHz (the relative bandwidth is 13.9%), which are similar to the simulated ones. The main difference between the tested and simulated results in Figure 1 is a deviation less than 250MHz, which is merely 5 percent of the center frequency of the design. As a consequence, the deviation is within the simulation error range. In terms of printed antennas, the reasons and results for the differences between simulated and tested results are as follows: (1) The unstable dielectric constant and the lossy, dispersive characteristics of dielectric substrates have effects on the accuracy of tested results of reflection coefficient as well as gain, leading to bandwidth migration together with a decrease of gain value. (2) The inhomogeneity of dielectric substrates also has influences on the antenna pattern, causing migration of its lobe. However, it has no appreciable effects on the pattern on H-plane but the E-plane tested in the article. (3) The discreteness of welding SMA connector also affects pattern and reflection coefficient of the antenna.

Simulated results on antenna gain are shown in Table 1. When compared with the results, although tested results are relatively small, they differ little. The tested results and simulated results suggest that, the out-of-roundness on H-plane for the frequency range from 4.6 to 5.0 GHz is less than 2 dB and the maximum gain is higher than 6 dB.

Comparing the design with antennas in literatures according to

Table 1. Tested results of gains of the antenna presented in the paper.

Frequency (GHz)	4.6	4.7	4.8	4.9	5.0
Tested value (dB)	4.0	5.6	5.9	6.0	6.1
Simulated value (dB)	4.3	6.0	6.4	6.4	6.4

Table 2. Comparison between antennas in this paper and other literatures.

Antenna Type	Working Bandwidth (GHz)	Relative Bandwidth (%)	Gain at Typical Frequency (dB)	Antenna Size (Electriclength)	Omni-directional Gain per Wavelength at Typical Frequency K
The antenna presented in this paper	4.35–5.0	13.9	5.9 (4.8GHz)	96.1mm×14.8mm×1.5mm (1.54λ×14.8mm×1.5mm)	3.8 dBi/λ
The antenna in [7]	3.32–3.77	12.7	6.4 (3.5GHz)	211mm× ϕ12mm (2.46λ×ϕ12mm)	2.6 dBi/ λ
The antenna in [8]	3.3–3.62	9.2	8.4 (3.5GHz)	353.5mm× ϕ13mm (4.12λ×ϕ13mm)	2.0 dBi/λ
The antenna in [9]	5.68–5.95	4.6	10 (5.8GHz)	300mm×15.2mm×2mm (5.80λ×15.2mm×2mm)	1.7 dBi/λ

the degrees of bandwidth, gain, and electrical per-unit-length gain K, where K is computed by formula (1), we can conclude that the greater value K is, the higher omni-directional gain of antennas generated by electrical per-unit-length is. That is, when meeting requirements of constant gain value, electrical size of antennas is expected to be smaller. So K can serve as a reference standard to compare miniaturization effects among different kinds of antennas.

$$K = \frac{G}{L}\lambda \tag{1}$$

In the formula, G — the linear value of antenna working at frequency point f, L — the length of antenna, λ — the wavelength in free space corresponding to frequency point f.

Table 2 presents results of comparison between antennas proposed in the paper and the ones in literatures. The results show that with its relatively wide bandwidth, the value K of the design is the greatest, also reaching equilibrium according to three indexes of bandwidth, gain, and size.

5. CONCLUSION

A composite dipole antenna array with direct feed is presented, meeting the requirements of wide bandwidth, high gain and omni-directional characteristics. And the structure of this design consists of a doublet antenna and an elliptic loaded monopole antenna with a skirted dipole. A good agreement between simulated results by CST Microwave Studio® and tested results suggest that the working frequency ranges between 4.35 to 5.0 GHz and the relative bandwidth can be 13.9%. Moreover, when working for the frequency range from 4.6–5.0 GHz, the out-of-roundness of the antenna pattern on H-plane is better than 2 dB, together with its gain at maximum radiation direction being 6.4 dBi as well as omni-directional gain generated by electrical per-unit-length being about 4 dB, which reaches the equilibrium concerned with indexes of bandwidth, gain, and size.

ACKNOWLEDGMENT

The authors would like to express their sincere gratitude to the funds supported by "the Fundamental Research Funds for the Central Universities" (Grant No. HIT.NSRIF.2010096).

The authors would also like to thank CST Ltd., Germany, for providing the CST Training Center (Northeast China Region) at our university with a free package of CST MWS software.

REFERENCES

1. Yang, G., Q.-X. Chu, et al., "Compact printed dipole antenna with integrated wideband balun for UWB application," *Microwave and Millimeter Wave Technology (ICMMT)*, 1–4, May 5–8, 2012.
2. Lin, S., J. H. Qiu, et al., "The simulation research of a novel UWB triangle monopole antenna," *International Conference on Antenna Theory and Techniques*, 256–258, Sept. 17–21, 2007.
3. Lizzi, L., G. Oliveri, P. Rocca, and A. Massa, "Planar monopole UWB antenna with UNII1/UNII2 wlan-band notched characteristics," *Progress In Electromagnetics Research B*, Vol. 25, 277–292, 2010.
4. Chayono, R., M. Haneishi, and Y. Kimura, "Inverted triangle printed monopole antenna with halfdisk for UWB applications," *Proceedings of Asia-Pacific Microwave Conference*, 1994–1997, Dec. 12–15, 2006.
5. Thanormsuay, S., P. Thosdee, and C. Thongsopa, "Array of quasi-rhomboid antenna for ultra wideband applications," *Proceedings of ECTI-CON*, 293–296, 2008.
6. Ren, Y.-J., C.-P. Lai, et al., "Compact ultrawideband UHF array antenna for through-wall radar applications," *IEEE Antennas and Wireless Propagation Letters*, Vol. 8, 1302–1305, 2009.
7. Zuo, S. L., Y. Z. Yin, Z. Y. Zhang, and X. Yang, "A design method to acquire high gain for omni-direction radiation applied in WiMAX," *Wireless Communications Networking and Mobile Computing*, 1–4, Sept. 24–26, 2009.
8. Zhang, Z. Y., G. Fu, S. X. Gong, S. L. Zuo, and T. Ran, "Printed 6-element dipole array antenna for omnidirection applied in WiMAX," *Wireless Communications Networking and Mobile Computing (WiCOM)*, 1–4, Sept. 23–25, 2010.
9. Chen, X., K. Huang, and X.-B. Xu, "A novel planar slot array antenna with omnidirectional pattern," *IEEE Transactions on Antennas and Propagation*, Vol. 59, No. 12, 4853–4857, Dec. 2011.